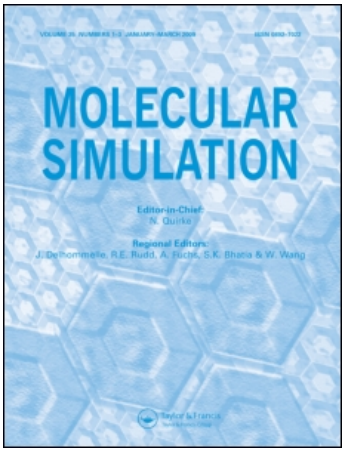

Molecular Simulation
Publication details, including instructions for authors and subscription information:
http://www.informaworld.com/smpp/title~content=t713644482

Statistical mechanics of fluids adsorbed in wedges and at edges

J. R. Henderson[a]
[a] School of Physics and Astronomy, University of Leeds, Leeds, UK

To cite this Article Henderson, J. R.(2005) 'Statistical mechanics of fluids adsorbed in wedges and at edges', Molecular Simulation, 31: 6, 435 — 448
To link to this Article: DOI: 10.1080/08927020412331332703
URL: http://dx.doi.org/10.1080/08927020412331332703

Molecular Simulation, Vol. 31, Nos. 6–7, 15 May – 30 May 2005, 435–448

Taylor & Francis
Taylor & Francis Group

Statistical mechanics of fluids adsorbed in wedges and at edges

J.R. HENDERSON

School of Physics and Astronomy, University of Leeds, Leeds LS2 9JT, UK

(Received September 2004; in final form September 2004)

Some of the history and modern significance of wetting phenomena involving wedge and edge geometries is discussed. The adsorption of fluids onto structured surfaces or colloidal objects yields rich behaviour, including new classes of interfacial phase transitions and alternative ways to consider classical capillarity. I describe how the equilibrium properties of these systems can be described with exact virial theorems obtained from statistical mechanics, that are of immediate relevance to computer simulation procedures, density functional theories and experiments capable of measuring inhomogeneous fluid density profiles. In wedge geometry the physics behind these sum rules can be illustrated with the use of the Derjaguin approximation, familiar to colloidal science. Three specific examples of the utility of statistical mechanics to this field are described: (i) a sum rule analysis is provided of capillarity phenomena involving two-phase coexistence within a linear triangular wedge, whose walls could be chemically distinct, (ii) an example emphasizing that experimental systems will typically involve both wedge and edge geometries that cannot be readily separated and (iii) an example concerning adsorption within an annular wedge, taken from colloidal science.

Keywords: Wetting; Adsorption; Contact angle; Wedges

1. Introduction

Nanoscience is often concerned with substrates patterned or structured on the nanoscale (intelligent surfaces) or the directed self-assembly of nanoparticles in solution or at solvated substrates. Although realizing the full potential of such systems will require the understanding of non-equilibrium behaviour at the nanoscale, the equilibrium structures formed are already very rich, controlled by interfacial phenomena in complex geometries. The role of geometry at the nanoscale is generic, such as super-hydrophobic substrates [1,2], the depletion attraction of colloidal science [3,4], including lock and key steric interactions [5], contact angle hysteresis [6,7], and interfacial phase transitions controlled by geometry [8]. Computer simulation procedures are ideally suited to the nanoscale, which is big enough to allow for smoothing of atomic detail, but small enough to be computationally efficient. However, simulations and also numerical density functional theories require a statistical mechanical framework with which to collect and analyse the data and to confirm the correctness of the procedures. Traditionally, this framework has been developed in semi-infinite planar geometry [9]. Thus, nanoscience provides a challenge to theoreticians to extend classical statistical mechanics to many-body systems interacting within complex geometries. This paper is exclusively concerned with exact results obtainable from realistic many-body hamiltonians in the presence of structured substrates defined by a one-body (external) field. In the remainder of this section, I consider some of the early history of liquid state physics, of direct relevance to modern approaches. In particular, I aim at a unified theme based on the significance of geometry. In Section 2, virial theorems that link the thermodynamic properties of fluids adsorbed in wedges (and at edges) to the density profile structure of the adsorbed fluid are described, together with new succinct derivations of recently published work [10]. This includes a virial theorem for Young's contact angle, necessary to yield two-phase coexistence within wedge geometry. Section 3 analyses these sum rules with the Derjaguin approximation familiar from colloidal science [3]. In Section 4, a sum rule analysis of capillarity (two-phase coexistence) within linear grooves whose walls are chemically distinct is carried out. Section 5 considers a solvated wedge-shaped nano-colloid. At first sight this object appears to be a "flying" wedge, due to unbalanced forces, however, careful attention paid to the inevitable association of edges with wedges restores physically acceptable behaviour. This issue has a wide experimental significance [11], linked with the definition of line adsorption and line tension (Appendix). In section 6, an example based on annular wedge geometry is considered, as is relevant to the surface forces apparatus and colloidal

Molecular Simulation
ISSN 0892-7022 print/ISSN 1029-0435 online © 2005 Taylor & Francis Group Ltd
http://www.tandf.co.uk/journals
DOI: 10.1080/08927020412331332703

depletion interactions. Finally, Section 7 concludes with a discussion emphasizing the relevance of equilibrium statistical mechanics to much of the exotic interfacial phenomena that has been/will be encountered in nanoscience.

The fact that substrate geometry can have dramatic significance to fluid interfacial phenomena has been known for a long time. For example, the first edition (1930) of the monograph by Adam [1] contains an explicit discussion of the physics of superhydrophobic surfaces, that would not require alteration for current publication, apparently surmized from early experiments in the 1920s. In figure 1 the physical content of Adam's argument is sketched. An otherwise planar substrate has been patterned in a series of triangular-shaped grooves, such that at liquid–gas coexistence the grooves have filled with gas, almost to the top of the wedges. This requires Young's contact angle θ of the liquid at the wedge walls to be equal to or greater than $(\pi + \beta)/2$ where β denotes the opening angle of the grooves (this condition is shown as an equality in the figure), which can be readily achieved for acute wedges. The excess liquid placed on top of the substrate is thus sitting almost entirely on gas and so the observed contact angle on the substrate will be close to π. Due to the ubiquitous presence of dispersion interactions and the inevitable sign of the associated Hamaker constant, this is the only class of system that shows superhydrophobic behaviour in nature (in the natural world unstructured planar solid–liquid interfaces do not approach complete drying).

In 1936, Wenzel [12] generalized the arguments of Young [13], to provide a thermodynamic description of the wetting of grooved, or rough, surfaces. However, Wenzel assumed that the adsorbed film follows the surface topology, rather than filling in the valleys to restore planar symmetry (as in figure 1). The transition between Wenzel's regime and Adam's regime is known as a filling transition; in the case of figure 1 this is filling by gas, while more typically one would observe filling by liquid at a grooved substrate–gas interface. The thermodynamic description of filling by gas at a superhydrophobic surface in contact with liquid was supplied in 1944 by Cassie and Baxter [14]; this work was funded by a UK government research institute devoted to the study of wollen materials (nicknamed WIRA) and the theme of this important paper could be described as a comparison between duck feathers and wool. Cassie and Baxter give due credit to Adam, but quote the 1938 edition thereby giving a slightly misleading impression of the chronology involved in the development of these ideas. Four years later, Cassie generalized this work to encompass the wetting of a chemically patterned planar surface; he assumed by direct analogy with figure 1 that the interfacial free energy is a simple average of independent contributions from the chemically distinct surface regions and thus arrived at Cassie's law [7]. Cassie's law predicts that the wetting of a chemically patterned surface can never be complete ($\theta = 0$) unless the liquid completely wets every chemically distinct region. When this condition is not met Cassie's picture corresponds to adsorbed liquid in the form of hemi-drops, with the three-phase contact lines pinned at or near the chemical pattern boundaries; here the observed contact angle is controlled by the geometry and is not equivalent to Young's contact angle. To generate complete wetting on such a surface the adsorbed liquid film must first unbend to wet the low energy regions; thereby violating Cassie's law but restoring Young's equation. This transition is somewhat analogous to filling and is known as an unbending transition [15] or more generally as an example of a morphological phase transition [16].

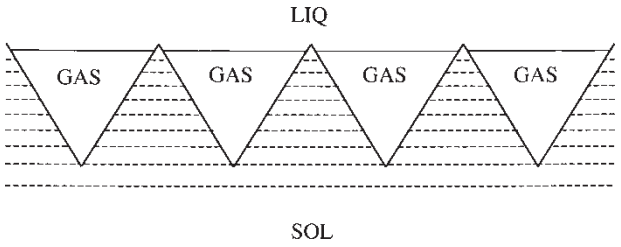

Figure 1. An example of a superhydrophobic surface. A solvophobic substrate has been grooved in a series of linear wedges. When excess liquid is placed on this substrate, in equilibrium with gas, the wedges remain filled with gas so that liquid is almost entirely in contact with gas. Hence the solid–liquid interface is very close to complete drying.

Cassie's law is one explanation of contact angle hysteresis [7], somewhat different to that which can be based on the earlier work of Wenzel [12]. In 1948, Shuttleworth and Bailey [6] returned to Wenzel's approach, to provide a thorough analysis of the spreading of a liquid over a grooved substrate. In this work, one finds the condition for the filling of a linear triangular wedge by liquid, at gas–liquid coexistence,

$$\theta = (\pi - \beta)/2. \tag{1}$$

For non-zero contact angles less than this value, saturated liquid will rise up the apex of a vertical wedge limited only by gravity even though the liquid does not completely wet the wedge walls, analogous to but different from capillary rise. In this context, filling was rediscovered in 1969 as a possible explanation of fluid transport in tall trees [17].

Recent work has emphasized that filling and unbending are examples of interfacial phase transitions. An approach to complete filling of a wedge from below saturation, analogous to an adsorption isotherm on a planar surface, is an example of interfacial critical phenomena [18,19]. Parry and coworkers [8] have emphasized remarkable theoretical predictions if the phase transition at the filling condition (1) is continuous: critical filling (see below). Fluctuation physics is especially significant because the long-wavelength modes are low-dimensional (quasi one-dimensional in the case of a linear wedge). Since the geometry of the structured substrate (e.g. the wedge angle β) plays the role of a key thermodynamic field, these transitions could be classified as geometrical wetting transitions. In fact, it is important to realize that it is geometry that distinguishes the various members of our expanding zoo of interfacial phase transitions. To illustrate

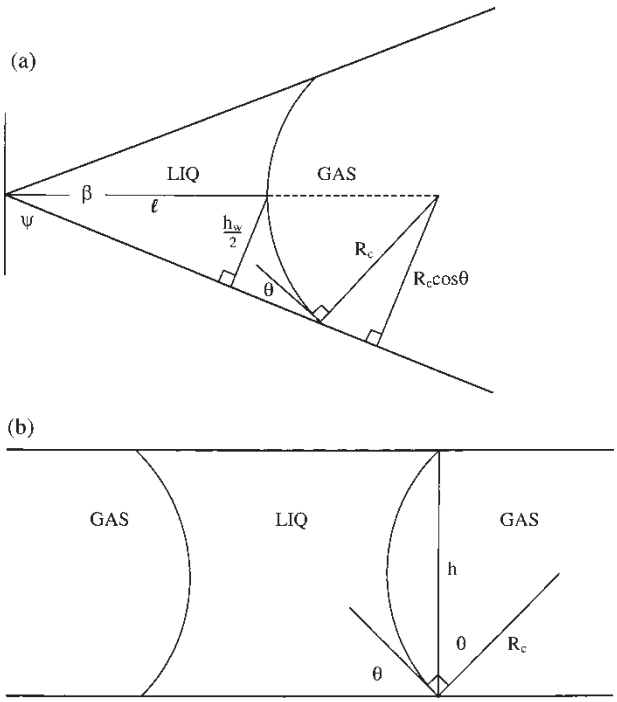

Figure 2. A comparison between (a) an approach to complete filling of a triangular wedge and (b) capillary condensation in a planar slit pore. In both cases mechanical equilibrium requires that the liquid–gas interfaces form an arc of radius of curvature R_c. This implies, for the two geometries, (a) $R_c \cos\theta = (\ell + R_c)\cos\psi$, (b) $h = 2R_c \cos\theta$.

this theme, it is instructive to consider the similarities and differences between filling, complete wetting and capillary condensation. Figure 2(a) sketches an approach to complete filling ($0 < \theta < \psi$) in a linear triangular wedge, while figure 2(b) shows condensation of a liquid bridge at the capillary condensation transition of a planar slit pore. An approach to complete wetting is defined as the continuous growth of a planar film at a planar wall (figure 2(a) at $\psi = \theta = 0$). In all three cases one is approaching saturation from low pressure and observing the growth of liquid films at surfaces. At first sight, one might imagine that filling is nothing other than capillary condensation up to the amount ℓ corresponding to the pore width h at the capillary condensation transition. To aid this comparison figure 2(a) defines the quantity h_w, which acts as an effective wedge width at an amount of filling ℓ. From the basic geometries sketched in figure 2, we have

$$h_w = 2R_c(\cos\theta - \cos\psi), \tag{2}$$

$$h = 2R_c\cos\theta, \tag{3}$$

where mechanical stability can be expressed as Laplace's equation, linking the liquid–gas interfacial radius of curvature R_c with the pressure difference Δp across the curved interface and its surface tension γ_{LG} : $R_c = \gamma_{LG}/|\Delta p|$. Thus, for a given isotherm and hence fixed contact angle $\theta(T)$, all the quantities h_w, h, ℓ, R_c diverge as $|\Delta p|^{-1} \rightarrow [1/(\rho_L - \rho_G)]|\delta\mu|^{-1}$ in the approach to saturation; ρ denotes a bulk density and saturation is reached at $\delta\mu = 0$ where μ denotes chemical potential. For very acute wedges ($\psi \rightarrow \pi/2$) the values of h_w and h even become identical, as if an acute wedge was nothing more than a slowly varying distribution of slit pores. However, this result is misleading because one must note that figure 2(b) holds only at a single value of $\delta\mu$, defining a first-order phase transition, whereas figure 2(a) holds for arbitrary bulk pressure in the approach to saturation, yielding a continuous interfacial phase transition ($\ell \sim |\delta\mu|^{-1}$ and thus the order-parameter critical exponent is unity).

The continuous nature of an approach to complete filling is in fact more appropriate to comparison with an approach to complete wetting on a planar surface. However, there are at least two geometric differences that distinguish these two continuous interfacial phenomena on a qualitative level. Firstly, the contact angle θ must be zero for an approach to complete wetting, while it is finite in the case of filling, and secondly, the dominant fluctuations associated with these examples of critical phenomena are two-dimensional in the case of wetting but one-dimensional for the filling of a linear wedge. Parry and coworkers [8] have emphasized that this latter issue is particularly relevant at a critical filling point (the special transition at $\theta = \psi_+$ controlled by higher-order contributions to the interfacial free energy arising from intermolecular forces). Similarly, critical filling shares attributes with critical wetting (a continuous variation of $\cos\theta \rightarrow 1_-$ at saturation), but they are qualitatively distinguished by the different dimensionality of the dominant fluctuations† [20]. In summary, although filling, wetting and capillary condensation are closely related interfacial fluid phenomena, it is clear that they acquire qualitatively different physics from the different geometries that are required to define them. More generally, it is equally clear that geometry plays a dominant role in nanoscience.

2. Virial theorems for wedge and edge geometries

Previous work has identified three exact virial theorems that relate interfacial thermodynamic quantities important to wedge and edge systems to the density profile structure induced by the wedge/edge walls; the wedge sum rules together with a virial theorem for Young's contact angle [10]:

$$\gamma = -\tan(\beta/2)\int_0^\infty \mathrm{d}t\,[\bar{p}(t) - p]_\beta, \tag{4}$$

$$\frac{\partial\tau}{\partial\beta} = -\int_0^\infty \mathrm{d}t\; t[\bar{p}(t) - p]_\beta, \tag{5}$$

$$\gamma_{LG}\sin\theta = -\int_{R_-}^{R_+} \mathrm{d}t[\bar{p}(t) - p]. \tag{6}$$

†Readers should perhaps be warned that neither of these two theoretically fascinating examples of interfacial critical phenomena have yet been unambiguously identified experimentally. Critical filling has, however, been successfully studied by computer simulation of short-ranged models, in contrast to the situation with critical wetting which appears to suffer from the marginal nature of the interfacial fluctuations at wetting (i.e. two-dimensional rather than quasi one-dimensional); see ref. [20]

The thermodynamic quantities appearing on the left of these sum rules are defined from the Grand potential Ω of a fluid adsorbed in a wedge, or at an edge, via the decomposition

$$\Omega \equiv -pV + 2\gamma A + \tau L_y. \tag{7}$$

Here, p denotes the bulk pressure (far from the wedge apex), V is the volume occupied by the coordinates of the fluid particles, γ is the wall–fluid surface tension (far from the wedge apex) and A is the surface area of each of the planar walls making up the wedge (a triangular wedge). The wedge is linear (along the y direction) and thus τ is a line tension (the excess Grand potential due to the presence of the wedge apex). In an approach to complete filling of a wedge, where a mesoscopic/macroscopic amount of liquid has condensed in the groove, the integrals on the right side of sum rules (4) and (5) include a nanoscopic range (between R_- and R_+) over which a liquid–vapour interface intersects the wedge walls. In this circumstance either of the first two sum rules can then be used to derive sum rule (6), which is a virial theorem for Young's contact angle expressing force balance normal to a planar wall (cf. Young's equation which expresses force balance along a planar substrate) [10]. Since this result belongs to the thermodynamic limit close to filling, where R_- is arbitrarily large, it follows that the wedge geometry is no longer relevant (hence the integrand has dropped the subscript β, the opening angle of the wedge, to emphasise that the result applies equally to a semi-infinite planar wall–fluid interface). In Section 4 below, this extension of classical capillarity is generalized to triangular wedges whose walls are chemically distinct.

The integrands on the right sides of all three sum rules are defined by the average normal pressure $\bar{p}(t)$ acting on the walls at a distance t from the wedge apex. For a wall–fluid model, where the wedge geometry is defined by an external field $v(\mathbf{r})$ acting on the fluid particles, this quantity is the ensemble averaged force per unit area acting on the wedge walls:

$$\bar{p}(t) = -\int_{-\infty}^{\infty} \mathrm{d}s \rho(s,t) v'(s), \tag{8}$$

where $\rho(s,t)$ is the one-body density profile in a coordinate system perpendicular (s) and parallel (t) to a wedge wall; see below. The wedge sum rules and the virial theorem for Young's contact angle are all members of the same class of virial theorem as the famous result linking the bulk pressure to the density at a semi-infinite hard-wall boundary, $p = kT\rho_w$ with k Boltzmann's constant and T the temperature; for a hard-wall wedge $\bar{p}(t) = kT\rho_w(t)$.

The wedge sum rules were first discussed in the context of hard-wall boundary conditions [21,22], then for a general wall–fluid potential $v(s)$ where the coordinate s varies perpendicularly to a specified wall [10]. This published work contains detailed derivations and discussion from a variety of routes, but it is possible to give succinct derivations that go directly to the desired sum rules in the general case. These powerful but perhaps sweeping general arguments are supplied here (readers desirous of additional rigour can turn to the earlier literature).

Sum rule (4) is a generalization of early work restricted to right-angled wedges and hard-wall boundary conditions [23,24]. To understand this result all that is required is to consider a many-body system confined within (wedge sum rule), or surrounding (edge sum rule), the triangular box drawn in figure 3(a). At the top right of this system is a linear wedge of opening angle β. In the thermodynamic limit this wedge becomes isolated from the other boundaries and hence can be considered to be a single isolated wedge of infinite depth, defined by a Grand ensemble (the whole system could also be taken to be a Grand ensemble but in the wedge case is more naturally a Canonical ensemble). For a general wall–fluid potential, a wedge/edge model is defined to belong to the infinite set of systems obtained from the intersection (at angle β) of any two semi-infinite planar wall–fluid models. This definition over counts some solid–fluid intermolecular interactions (in the wedge model arising from the solid region defined by the fluid wedge reflected into the solid) in order to enforce strict wedge geometry for every isopotential of the wall–fluid interaction. One should be aware that this is an idealization of true molecular models, which will not preserve this strict geometric condition at

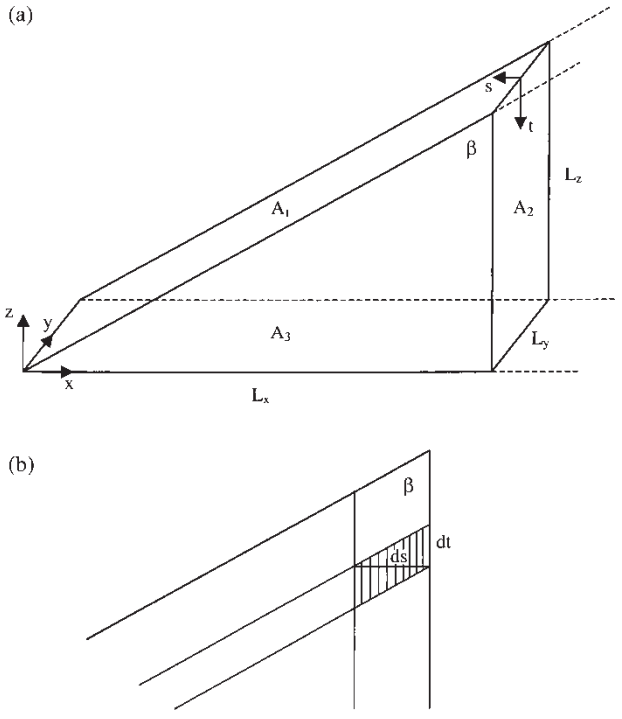

Figure 3. System geometry used for the derivation of linear wedge/edge virial theorems. Part (a) could be regarded as the boundary of a computer simulation system, either filled with fluid (the wedge sum rule) or surrounded by fluid (the edge sum rule). The wedge/edge of interest is labelled by its opening angle β. Note that with an appropriate modification of the left side of the system ($x = 0$) it would be a trivial matter to incorporate obtuse angles into the construction (the wedge/edge sum rules apply for all $0 < \beta < \pi$). Part (b) depicts the coordinate system appropriate to a strict wedge/edge model (all wall–fluid isopotentials possess identical geometry); i.e. $\mathrm{d}\mathbf{r} \equiv \mathrm{d}t\,\mathrm{d}s\,\mathrm{d}y$.

the very apex of a physical wedge. One should also note that the isopotentials drawn in figure 3 and elsewhere are wall–fluid interaction boundaries, not physical boundaries. When fluid lies outside the body drawn in figure 3(a), the edge model, the relationship to physical systems is even less realistic since not even the rolling of a hard-sphere around a sharp linear edge will generate a sharp edge model [25]. Notwithstanding these comments, which amount to the impossibility of defining a generic wedge or edge model appropriate to general intermolecular interactions (at the molecular level), it is nevertheless important to develop statistical mechanical methods appropriate to wedge/edge geometry. My choice enforces this geometry to the extreme limit, but other models can be treated in precisely the same manner to yield related virial theorems, although they will not be so easily understood in terms of the defining geometry.

Let us now consider the change in the Grand potential of a fluid contained within the boundary walls of figure 3(a), when the system is uniformly extended in the x-direction; $L_x \rightarrow L_x + \partial L_x$. This process leaves the wedge of interest completely unchanged, but it does increase the volume of the system, the surface areas of all the boundary walls and the lengths of all the linear wedges not aligned with the y-axis. The latter higher-order free energy changes are not considered (although they do lead to a sum rule for the line tension of these $\pi/2$ wedges in terms of the interfacial structure in a corner [24]). Rather, to leading-order in interfacial quantities, this virial process leads to a sum rule for the wall–fluid interfacial tension γ of the walls forming the β wedge (walls A_1 and A_2), all the other interfacial contributions concern $\pi/2$ wedges and can be ignored. Concentrating purely on the wedge of interest we have

$$\partial\Omega_\beta^{\mathrm{ex}} = \gamma(\partial A_1 + \partial A_2), \tag{9}$$

where the superscript ex denotes an interfacial property (without the bulk pV contribution to the Grand potential) and (in this section) the chemical properties of walls A_1 and A_2 are assumed to be identical. For any wall–fluid model it is possible to calculate the left side of equation (9) directly from the partition function [26],

$$\frac{\partial\Omega}{\partial L_x} = \int \mathrm{d}\mathbf{r}\rho(\mathbf{r})\frac{\partial v(\mathbf{r})}{\partial L_x}. \tag{10}$$

My strict choice of wedge model allows for the use of the coordinate system sketched in figure 3(b), where t is a coordinate that moves parallel to the wall A_2, down from wall A_1, and s measures the perpendicular distance outwards from wall A_2; note that the virial process under consideration only moves wall A_2 so it is only the external field produced by this wall that will enter the sum rule. When this coordinate system is introduced into equation (10) we obtain

$$\frac{\partial\Omega_\beta^{\mathrm{ex}}}{\partial L_x} = L_y\int_0^\infty \mathrm{d}t\int_{-\infty}^{\infty}\mathrm{d}s[\rho(s,t) - \rho^\pi(s)]v'(s). \tag{11}$$

Hereafter the quantity $\rho^\pi(s)$ denotes the density profile induced by a planar semi-infinite wall (i.e. the integrand of equation (11) tends to zero away from the apex); this quantity has been introduced to cancel the volume term in $\partial\Omega$ and so leave a sum rule for $\partial\Omega_\beta^{\mathrm{ex}}$ alone. Since $A_1 = L_xL_y/\sin\beta, A_2 = L_xL_y/\tan\beta$, and simple trigonometry gives $1/\sin\beta + 1/\tan\beta = 1/\tan(\beta/2)$, when equation (9) is equated with equation (11) one is led immediately to sum rule (4), with $\bar{p}(t)$ identified as in equation (8); note also that $\bar{p}(t) \rightarrow p$, the bulk pressure, as soon as t is large enough to ensure $\rho(s,t) \rightarrow \rho^\pi(s)$.

To derive sum rule (5), we require only the construction of figure 4. This diagram, which is enlarged beyond the infinitesimal changes required, shows the infinite wall–fluid boundaries (full lines) and a single attractive wall–fluid isopotential of one wall being rotated about the apex (dashed lines), before and after the wedge angle has been increased by an amount $\mathrm{d}\beta$. The same coordinate system of figure 3(b) can be used; in particular, for this process

$$\mathrm{d}v \equiv v(s + \mathrm{d}s) - v(s) = \mathrm{d}s\,v'(s) = \mathrm{d}\beta t v'(s). \tag{12}$$

One can then evaluate the change in Grand potential; cf. (10):

$$\frac{\partial\Omega}{\partial\beta} = L_y\int_0^\infty \mathrm{d}t\int_{-\infty}^{\infty}\mathrm{d}s\rho(s,t)\frac{\partial v(s)}{\partial\beta}, \tag{13}$$

so that on comparison with the definition (7) and, as usual, removing the contribution from the volume change (note that there is no change in interfacial area

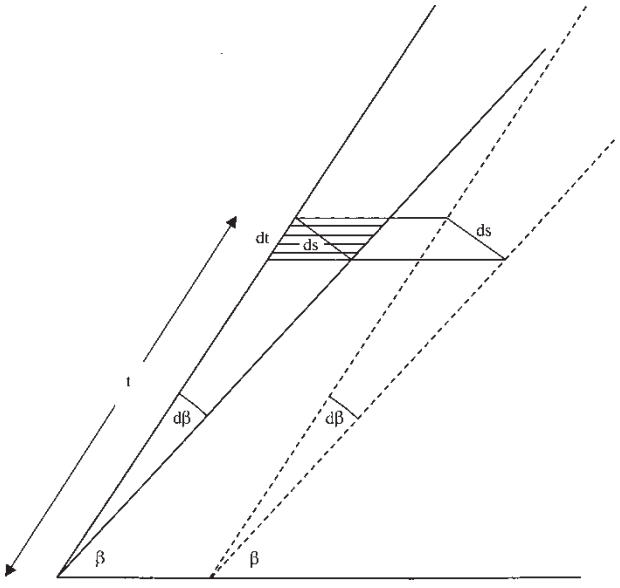

Figure 4. System geometry used to derive a virial theorem for the solvation torque acting on a solvated linear wedge/edge. Thick solid lines denote the boundaries of infinite wall–fluid repulsion. The dashed lines depict an attractive wall–fluid isopotential of a boundary wall that is being rotated about the apex of the wedge/edge. The same coordinate system as figure 3(b) is depicted, but note that for this construction $\mathrm{d}s = t\mathrm{d}\beta$.

for this process) we have

$$\frac{\partial \tau}{\partial \beta} = \int_0^\infty dt t \int_{-\infty}^\infty ds[\rho(s,t) - \rho^\pi(s)]v'(s) \qquad (14)$$

$$= -\int_0^\infty dt t[\bar{p}(t) - p]_\beta. \qquad (15)$$

Identical derivations hold for the edge model, except that $dv(s)$ now picks up a minus sign due to the change in geometry associated with fluid occupying the space outside the bodies drawn in figure 3(a) and figure 4, rather than inside. Thus, if we are prepared to accept the somewhat unphysical nature of this strict edge model, particularly for acute edges and close to the planar limit (note that in contrast the strict wedge model is actually most physical for an acute wedge), then the edge sum rules are identical to equations (4) and (5) apart from there no longer being minus signs appearing on the right sides of both results.

3. Derjaguin analyses of the wedge sum rules

In colloidal science, it has long been a tradition to treat fluid "confined" within a wedge (such as the annular wedge formed by two large colloids in close proximity) by approximating the fluid mediated interaction across the wedge as the interaction obtained from an appropriate distribution of planar parallel pores; Derjaguin's approximation [3]. In this section, this approach is used to evaluate the wedge sum rules and the virial theorem for Young's contact angle.

Derjaguin's approximation for a wedge can be expressed in the form

$$\bar{p}(t) - p \rightarrow \Pi(h) \equiv -\partial\Phi(h)/\partial h, \qquad (16)$$

where $\Phi(h)$ is the fluid mediated interaction (free energy per unit wall area) due to the confinement of fluid within the planar pore (as drawn in figure 2(b) but without the presence of two-phase coexistence); note that $\Phi(\infty) \equiv 0$ and so $\Phi(0) = -2\gamma$ (when h is reduced from a macroscopic separation to the point where all fluid has just been expelled from the planar pore ($h = 0$) then the Grand potential of the pore system has changed by precisely two wall–fluid interfacial free energies; see equation (40) of the Appendix). I choose to define the equivalent of h in the wedge system with the construction of figure 5(a). This choice is clearly suited to acute wedges, where the density profile structure in the wedge will be dominated by the influence of the nearest side wall (profile structure oriented in the s-direction). This implementation of Derjaguin's approximation therefore replaces the true density distribution with two planar wall–fluid profiles that meet along the line of symmetry of the wedge. Repulsive fluid–fluid forces (on the scale of a diameter σ) transmitted along the path of length h will then manifest themselves along the wedge walls on a scale $\Delta t = \sigma/(2\tan(\beta/2)) \rightarrow \sigma/\beta$. This behaviour is known to hold for hard sphere fluid adsorbed in acute hard wedges [22], but is unphysical for $\Delta t < \sigma(\beta > 53°)$. Beyond this angle, correlations transmitted down the wall from the apex should start to dominate. Notwithstanding this caveat, when equation (16) is substituted into sum rule (4) one finds that this approximation satisfies the sum rule exactly, for arbitrary wedge angles $0 < \beta < \pi$:

$$\gamma \rightarrow -\frac{1}{2}\int_0^\infty dh\Pi(h) = -\frac{1}{2}\Phi(0). \qquad (17)$$

The conclusion one might draw from this astonishing result is that the Derjaguin approximation must in fact be exact in the limit of $\beta \rightarrow 0$ and that the constraints involved in satisfying sum rule (4) in this limit are sufficiently restrictive to prevent any deviation at non-zero wedge angles.

When Derjaguin's approximation equation (16) is substituted into sum rule (5) one obtains an explicit result

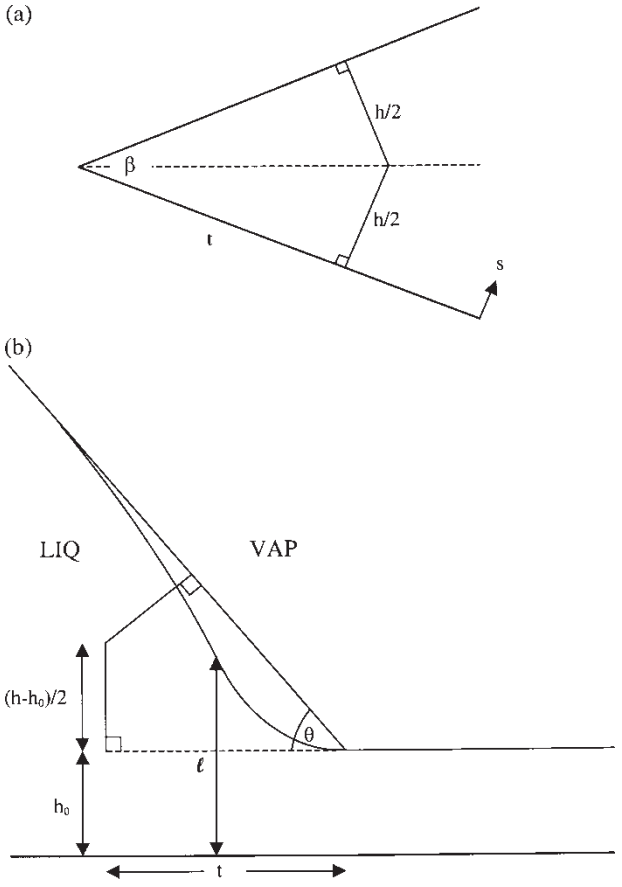

Figure 5. Coordinate systems defining Derjaguin analyses of (a) the wedge sum rules and (b) the virial theorem for Young's contact angle. (a) The path of length $h = 2t\tan(\beta/2)$ denotes the fluid mediated interaction between the walls of the wedge (treated as a distribution of semi infinite slit pores in the Derjaguin approximation). (b) A Derjaguin construction for analysing the mechanical stability of the wedge-shaped region defined by the intersection of a liquid–vapour interface with a planar wall–fluid boundary. The fluid-wedge of angle θ is defined by the extrapolation of the liquid–vapour interface far from the wall. Close to the wall, the true interface will distort under the influence of the wall–fluid interaction (the curve at height $\ell(t)$). The planar film of height h_0 is molecularly thin because θ is non zero.

for the line tension as a function of wedge angle:

$$-\frac{\partial\tau}{\partial\beta}\rightarrow\frac{1}{4\tan^2(\beta/2)}\int_0^\infty \mathrm{d}h h\Pi(h)\equiv\frac{W}{4\tan^2(\beta/2)}, \quad (18)$$

with $W=\int_0^\infty \mathrm{d}h\Phi(h)$ defined by the entire distribution of planar pores (a quantity familiar in colloidal science as the barrier to flocculation). This result integrates to give

$$\frac{\tau}{W}=\frac{1}{2\tan(\beta/2)}-\frac{\pi-\beta}{4}, \quad (19)$$

where the constant of integration has been chosen to ensure that τ is zero for a planar substrate ($\beta=\pi$); one expects τ to pass smoothly through zero as one moves from wedge to edge geometry. The limiting behaviour for acute wedges, $\tau\sim 1/\beta$, would appear to be an exact consequence of geometry (i.e. for rigid walls) [21]. Outside this limit the angle dependence predicted by equation (19) is likely to be an accurate representation of the unknown exact behaviour, but is presumably an approximation. The Derjaguin ansatz can also be applied directly to the Grand potential (and hence to τ) and this result deviates from equation (19) at large values of β; in fact, one expects the solvation torque $-\partial\tau/\partial\beta$ to be zero in the planar limit $\beta=\pi$, as well as τ, as predicted by equation (18) but not by the same approximation applied to the Grand potential [21]. This inconsistency is precisely what one anticipates from an approximation, in contrast to equation (17).

We can also apply the Derjaguin approximation to the flexible wedge formed by the intersection of a liquid–vapour interface with a planar wall, see figure 5(b). This approach has been used by Indekeu [27] to develop a theory of the line tension formed by a macroscopic drop adsorbed on a planar substrate (Young's system). Young's contact angle is defined by the idealized triangular wedge in figure 5(b), whereas the actual liquid–vapour interface is free to distort in the region close to the wall in order to minimize the total free energy; an interface displacement model (defined by $\ell(t)$ sketched in figure 5(b)). Clearly, this physics must be contained within the exact sum rule (6). The direct analogue of the Derjaguin approximation used in conjunction with the wedge sum rules is drawn in figure 5(b); this time one needs to take into account a nanoscopically thin film of liquid present at the wall–vapour interface. When inserted into sum rule (6) this approximation yields

$$\gamma_{\mathrm{LG}}\sin\theta\rightarrow-\frac{\alpha_d}{2\tan(\theta/2)}\int_{h_0}^\infty \mathrm{d}h\Pi(h), \quad (20)$$

or

$$1-\cos(\theta)\rightarrow-\frac{\alpha_d}{2}\frac{\Phi(h_0)}{\gamma_{\mathrm{LG}}}. \quad (21)$$

Here a distortion coefficient α_d is introduced, in an attempt to correct for the interface displacement that must be present. Equation (21) has the same structure as Frumkin–Derjaguin theory; in fact, choosing $\alpha_d=2$ leads to the identical result [28]. Accordingly, sum rule (6) contains the physics of the disjoining pressure within it, long ago developed by Frumkin and Derjaguin. Note that sum rule (6) is obtained from a macroscopic limit, where the difference between p_G and the saturation pressure is negligible; corrections allowing for a non-zero pressure difference across the liquid–gas interface and hence a macroscopic curvature would affect sum rule (6) only at the level of a Tolman length curvature correction to γ_{LG}. Similarly, nowhere in this paper is it necessary to distinguish between the values of γ_{LG} and γ_{LV}. This distinction is used to differentiate between an approach to saturation ($|\Delta p|$ small but non-zero) from the limit of bulk liquid–vapour coexistence ($|\Delta p|=0_+$).

We can also directly check the consistency of Indekeu's interface displacement model with sum rule (6), noting that the former was carried out in the regime where θ is small. Defining the interface potential $\psi(\ell)\equiv\Phi(\ell)-\Phi(h_0)$; hence $\psi(h_0)=0$ and $\psi(\infty)=-\Phi(h_0)\equiv -S$, where S is the spreading pressure; from the construction of figure 5b and inserting into sum rule (6), yields

$$\gamma_{\mathrm{LG}}\theta\rightarrow\int_{-\infty}^\infty \mathrm{d}t\frac{\partial\psi}{\partial\ell}=\int_{h_0}^\infty \mathrm{d}\ell\frac{\partial\psi/\partial\ell}{\partial\ell/\partial t}. \quad (22)$$

The formal solution to the interface displacement model, equation (2.6) of ref. [27], is the first integral $(1/2)\gamma_{\mathrm{LG}}(\partial\ell/\partial t)^2=\psi(\ell)$, which when substituted into equation (22) gives $\gamma_{\mathrm{LG}}\theta\rightarrow\sqrt{2\gamma_{\mathrm{LG}}\psi(\infty)}$ or $\psi(\infty)\rightarrow(1/2)\gamma_{\mathrm{LG}}\theta^2$ exactly as expected in the small contact angle regime.

4. Sum rule analysis of capillarity in non-symmetric wedges

In an approach to saturation beyond the filling condition an arbitrary amount of liquid can be adsorbed in a macroscopic wedge. In this situation, the line tension of the wedge picks up a contribution due to the presence of the liquid–gas interface lying far from the apex. When either sum rule (4) or (5) is applied to this situation, then one is lead to the virial theorem for Young's contact angle equation (6) [10]. In this section, the sum rule analysis is extended to incorporate linear wedges constructed from chemically distinct planar walls (non-symmetric triangular wedges). Capillarity and filling transitions in non-symmetric wedges have previously been discussed by Jakubczyk and Napiorkowski [29]. In the non-volatile limit they report the existence of mechanically stable bridge-like and drop-like (confined to one wall only) configurations, in addition to the obvious generalisation of figure 2(a) to encompass two contact angles θ_1 and θ_2; it is not clear if these exotic states can exist in true thermodynamic equilibrium, but if so, they are not considered here. Interesting issues that arise when applying the virial theorems of Section 2 to non-symmetric geometry is the focus of this Section. Note, in particular, that the generalization of sum rule (4) must involve two different

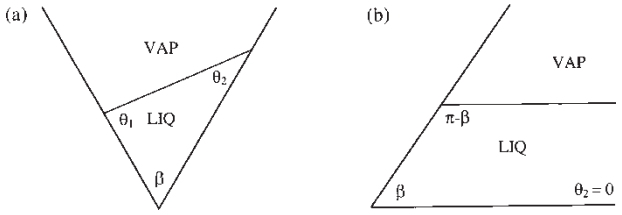

Figure 6. The filling condition for a triangular wedge with chemically distinct walls, that therefore induce different values of Young's contact angle; θ_1, θ_2. (a) When both walls are partially wet by saturated liquid, $\theta_1 + \theta_2 + \beta = \pi$. (b) When one of the walls is completely wet, $\theta_2 = 0$ and hence $\theta_1 = \pi - \beta$.

wall–fluid tensions γ_1 and γ_2, while the derivation leading to sum rule (5) must yield two equivalent sum rules (since it cannot matter which of the two chemically distinct walls is rotated to alter the wedge angle β).

In figure 6, the filling condition for non-symmetric wedges is sketched in two standard cases. Figure 6(a) (where neither wall shows complete wetting) has ignored Earth's gravity, while figure 6(b) (where only one of the walls is completely wet) is oriented correctly in this regard. At this condition, mechanical stability (a coupled pair of Young's equations) allows for an arbitrary filling of the wedge at saturation (zero macroscopic curvature on the liquid–gas interface). Defining the average contact angle $\bar{\theta} \equiv (\theta_1 + \theta_2)/2$ and the complementary wedge angle $\psi \equiv (\pi - \beta)/2$ as in figure 2(a), then an approach to complete filling will occur as the pressure is raised towards saturation provided $\psi > \bar{\theta}$; the analogue of the situation drawn in figure 2(a).

The virial procedure of Section 2 based on figure 3 can still be employed. Evaluating the changes in interfacial free energies of walls 1 and 2, associated with the top right wedge (of angle β), when L_x is increased by an infinitesimal amount exactly as before, and inserting into the general result equation (10), we arrive at the non-symmetric version of the first wedge sum rule:

$$\gamma_1 + \gamma_2 \cos\beta = -\sin\beta \int_0^\infty \mathrm{d}t[\bar{p}(t) - p]_{2,1}, \qquad (23)$$

where the subscript on the integrand reminds the reader that the integral must travel down wall 2, from the apex formed with wall 1. When the two walls are identical then this result reduces to equation (4) as it must. Now consider an approach to complete filling in the non-symmetric wedge at $\psi > \bar{\theta}$, where to leading-order in the macroscopic curvature we can set $\gamma_i = \gamma_{\mathrm{WL}_i} + \gamma_{\mathrm{LG}} \cos\theta_i$ from Young's equation applied arbitrarily far from the wedge apex (beyond the adsorbed liquid). Evaluating equation (23) directly, for this situation, yields

$$\begin{aligned}\gamma_{\mathrm{WL}_1} + \gamma_{\mathrm{LG}} \cos\theta_1 + (\gamma_{\mathrm{WL}_2} + \gamma_{\mathrm{LG}} \cos\theta_2)\cos\beta \\ = -\sin\beta \left\{ \int_0^{R_2} \mathrm{d}t[\bar{p}(t) - p_{\mathrm{L}}]_{2,1} + R_2 \Delta p \right. \\ \left. + \int_{R_{2-}}^{R_{2+}} \mathrm{d}t[\,\bar{p}(t) - p]_2 \right\}. \qquad (24)\end{aligned}$$

The first term on the right side, the only term present in the absence of two-phase coexistence in the wedge, cancels the wall–liquid tensions on the left side. The second term on the right side is given by Laplace's equation for this system ($\Delta p = -\gamma_{\mathrm{LG}}/R_{\mathrm{c}}$ where R_{c} is the radius of curvature of the liquid–gas interface) and the final term on the right side, which runs across the nanoscopic region in which the liquid–gas interface intersects the wall–fluid interface, is given by sum rule (6); i.e. the integral equates to $-\gamma_{\mathrm{LG}} \sin\theta_2$. Thus, when the non-symmetric wedge sum rule (23) is applied to an approach to complete filling in the wedge, we must have, for consistency with the symmetric case, the trigonometric identity

$$\cos\theta_1 + \cos\theta_2 \cos\beta = \sin\beta \left(\frac{R_2}{R_{\mathrm{c}}} + \sin\theta_2 \right). \qquad (25)$$

Precisely at filling, where $R_{\mathrm{c}} = \infty$, this identity reduces to $\theta_1 + \theta_2 + \beta = \pi$ as drawn in figure 6(a); the general case $\psi > \bar{\theta}$ is addressed after first considering the extension of sum rule (5).

It is not hard to see from the discussion of Section 2 that the torque virial theorem based on the construction of figure 4 applies automatically to a non-symmetric wedge. The only generalization is that one can move either wall in order to generate $\partial\tau/\partial\beta$ and hence one arrives at an equivalence between two wedge integrals, along different walls joined at the apex:

$$\int_0^\infty \mathrm{d}t t[\bar{p}(t) - p]_{2,1} = \int_0^\infty \mathrm{d}t t[\bar{p}(t) - p]_{1,2}. \qquad (26)$$

Note that it is only this particular moment of the disjoining pressure that equates for the two walls, it is not true for the zeroth moment that enters equation (23), nor for any other moment. When equation (26) is evaluated using sum rule (6) to leading-order in the interfacial curvature R_{c}^{-1}, in the approach to complete filling, it follows that

$$\frac{R_1^2}{2}\Delta p - R_1 \gamma_{\mathrm{LG}} \sin\theta_1 = \frac{R_2^2}{2}\Delta p - R_2 \gamma_{\mathrm{LG}} \sin\theta_2, \qquad (27)$$

which when combined with Laplace's equation implies a second trigonometric identity that must hold for the approach to filling of a non-symmetric wedge:

$$R_1^2 + 2R_1 R_{\mathrm{c}} \sin\theta_1 = R_2^2 + 2R_2 R_{\mathrm{c}} \sin\theta_2. \qquad (28)$$

From the above it follows that the identities (25) and (28) provide a direct check on the internal consistency of the three virial theorems discussed in this paper. The geometric proof of this consistency can be read off figure 7. The only physics assumed in this figure is that the liquid–gas interface forms part of an arc, of radius of curvature R_{c}; Laplace's equation. To prove identity (25) we need only note that the two parallel dashed lines in figure 7 are of equal length, thus

$$u + v = (R_2 + x)\sin\beta. \qquad (29)$$

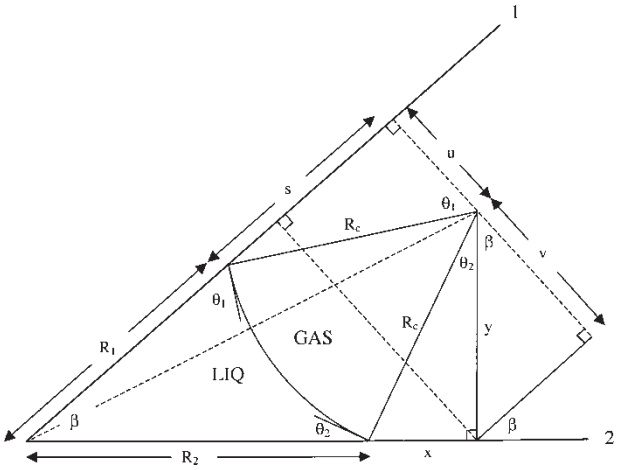

Figure 7. A geometric construction showing the consistency between the wedge sum rules and the virial theorem for Young's contact angle, with each other and with mechanical equilibrium as expressed by Young's and Laplace's equations. Physically, this represents an approach to complete filling in a non-symmetric triangular wedge. The key geometric quantities of interest are: $x = R_c \sin\theta_2$, $y = R_c \cos\theta_2$, $s = R_c \sin\theta_1$, $u = R_c \cos\theta_1$ and $v = y\cos\beta = R_c \cos\theta_2 \cos\beta$.

From the remaining dashed line in figure 7, the shared hypotenuse, we have

$$(R_1 + s)^2 + u^2 = (R_2 + x)^2 + y^2, \tag{30}$$

which leads quickly to the identity (28). This remarkable geometric construction is a nice example of "interfacial statistical geometry" [22].

5. Wedges combined with edges

The model of an isolated linear wedge/edge, infinite in all dimensions, is an idealized representation of subsystems found in nature. Palágyi and Dietrich [11] have recently stressed that typical experimental systems will contain wedges and edges that are inevitably linked together; e.g. machining a triangular wedge into a planar substrate must also create two edges, while a grooved substrate (figure 1) is a series of both wedges and edges. If a standard adsorption experiment was carried out on such a substrate then it would not be easy to extract, say, the line adsorption of a single isolated wedge. Furthermore, it turns out that the choice of boundary condition far from the wedge/edge apex of interest must in itself introduce further wedges (including "mathematical" wedges if the system is part of a simulation experiment). At first sight, this appears to introduce an arbitrariness into the definition of a line adsorption and hence line tension [11]. However, this difficulty is not a property of the sum rule analyses, since the integrands of the wedge/edge sum rules go rapidly to zero as soon as the integrals leave the region of influence of the apex ($\rho(s,t) \to \rho^{\pi}(s)$). Accordingly, any experiment sophisticated enough to measure the density profile as a function of distance along a wedge wall, such as a computer simulation experiment, must be able to measure a unique line adsorption and hence line tension associated with the single wedge or edge of interest. The Appendix below considers, which precise definition of line adsorption is associated with the line tension defined by the decomposition equation (7) and hence the line tension appearing in sum rule (5). In this section, the experimental significance of these related issues is illustrated in the context of the solvation of a wedge-shaped colloidal solute. This class of problem is potentially of some significance to nanoscience due to the importance of self-assembly driven by depletion interactions between colloidal objects and structured substrates or between each other [4]. This may even extend to the "lock and key" interactions of crucial importance in biology [5].

Consider a wedge-shaped colloidal object of triangular cross section, as sketched in figure 8. To focus on a potentially interesting phenomenon, it is assumed that the wedge walls are solvophobic, so that close to saturation a wedge-shaped bubble will form in the apex of the wedge (figure 8(b)). In computer simulation this system could be readily achieved by idealizing the walls as hard walls, since the interface between saturated liquid and a planar hard-wall is always dry (contact angle $\theta = \pi$). In the context of the wedge/edge sum rules this model reduces to the simple result $\bar{p}(t) = kT\rho_w(t)$, where the subscript w denotes the limiting value of the density profile on the hard boundary. Inserting a colloidal object into solvent generates a solvation force acting on the body as a whole:

$$\mathbf{F}^{\text{solv}} = -\oint \mathrm{d}\hat{s}[\bar{p}(t) - p], \tag{31}$$

where the bulk pressure term has been included for comparison with the sum rules; it contributes zero by symmetry (figure 8(a)). At first sight figure 8(b) raises the issue of an unbalanced solvation force, in this case in the z-direction; a "flying" wedge. Namely, for a hard-wall wedge ($\theta = \pi$) of length L the pressure difference across the curved liquid–gas interface sketched in figure 8(b) implies an upwards force of magnitude $2\Delta pxL = 2\gamma_{\text{LG}}Lx/R_c = 2\gamma_{\text{LG}}\text{L}\cos(\beta/2)$. In fact, we shall see

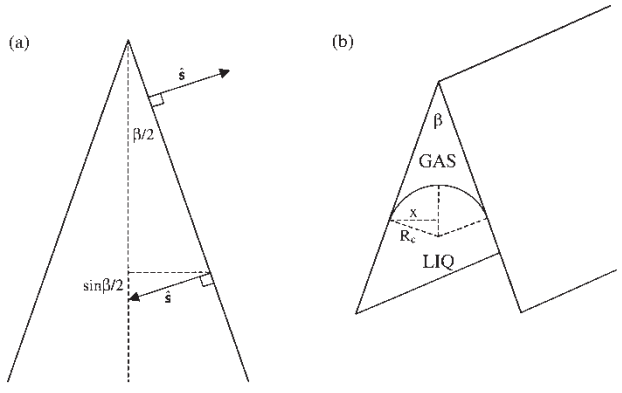

Figure 8. A linear wedge-shaped colloid particle, to be considered placed in solution. (a) Coordinate system for calculating the solvation force acting on the colloid body. (b) When the colloid walls are treated as hard-wall boundaries and the solvent approaches saturation, then a wedge-shaped gas bubble will form at the apex of the inner groove.

shortly that sum rule (4) applied to the inner wedge walls leads to precisely this result; since at drying $\gamma = \gamma_{WG} + \gamma_{LG}$ and the wall–gas contribution can be neglected (it actually contributes immediately at the wedge apex). When the outer edge integrals (one each side of the edge) are included the total unbalanced force in the z-direction is twice this amount ($\hat{s}$ changes sign but so does the sign in front of the sum rule). This disturbing result is given some credence by the obvious analogy of figure 8(b) with capillary rise, which is indeed unbalanced in the absence of Earth's gravity (as televised in space-station demonstrations).

Could such a colloidal object really "fly"? Common sense is restored, however, by the realization that we have been too sloppy with the depiction in figure 8. Instead, we need to remember that an isolated wedge/edge cannot exist in nature, rather, we should have drawn something along the lines of figure 9 where the arbitrarily sharp tails are now apparent. The force-balance on our colloidal wedge is equally concerned with the force on these tails. Again, symmetry alone tells us that we need to only consider the force acting along the line of symmetry (the z-direction). The surface integral in the definition of the solvation force equation (31) now runs over three edges as well as the inner wedge. In each case, we can make the translation $\oint \mathrm{d}\hat{s} \to L\hat{s} \int \mathrm{d}t$ where the $\hat{s}_z$ components of interest are given in figure 9. One can readily check that the bulk pressure term sums to zero as it must, since $t' \sin(\beta'/2) - t \sin(\beta/2) = d - d = 0$. The wedge and edge contributions can all be evaluated from sum rule (4), assuming a chemically homogeneous surface to our colloidal object. Namely,

$$\hat{s}_z \int \mathrm{d}\{t, t'\} [\bar{p}(t) - p]_{\beta,\beta'} \sim \frac{\sin(\beta/2)}{\tan(\beta/2)} - \frac{\sin(\beta/2)}{\tan(\delta/2)} + \frac{\sin(\beta'/2)}{\tan(\delta/2)} + \frac{\sin(\beta'/2)}{\tan(\beta'/2)}$$

$$= \frac{1}{\tan(\delta/2)} \{ \tan(\delta/2)[\cos(\beta/2) + \cos(\beta'/2)] - [\sin(\beta/2) - \sin(\beta'/2)]\} \quad (32)$$

$$= \frac{2}{\tan(\delta/2)} \left\{ \tan\left(\frac{\beta - \beta'}{4}\right) \cos\left(\frac{\beta - \beta'}{4}\right) - \sin\left(\frac{\beta - \beta'}{4}\right) \right\} \times \cos\left(\frac{\beta + \beta'}{4}\right) \quad (33)$$

$$= 0. \quad (34)$$

From the first line of the above proof one can see immediately by reference to the angles labelled in figure 9 which wedge and edge surfaces each term belongs to (the first is the sum of the wedge wall terms and the rest are edge contributions). It is essential to include all these contributions in order to understand the stability of this object immersed in solvent. When the colloid approaches a boundary wall, or another colloid, then additional wedges and edges are created (remember that the "walls" are actually wall–fluid repulsive boundaries). In these latter cases the solvation force on the colloid is unbalanced, leading to a so-called depletion interaction. For example, spherical colloids are trapped at the bottom of wedges and repelled by edges.

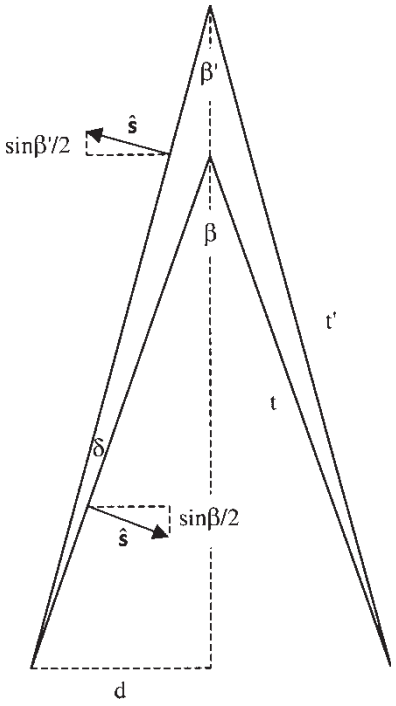

Figure 9. A physically correct depiction of the cross-section of the wedge-shaped colloid particle sketched in figure 8. Note that one cannot avoid the presence of the edge-shaped tails (internal angle $\delta = (\beta - \beta')/2$) no matter how long or how thin the walls are made.

6. Annular wedges

In colloidal science the wedge geometry of most significance is annular, rather than linear, as formed by two spherical colloids in close proximity, or when a spherical colloid approaches a planar wall (see figure 10). The geometry of figure 10 is also that relevant to the crossed-cylinder configuration of the surface forces apparatus [30]. The adsorption of hard sphere fluid in an annular wedge is somewhat controversial at present, due to an apparent discrepancy between the statistical mechanical formulation of Derjaguin's approximation and the results of fundamental-measure density-functional-theory (FMDFT) [4,31], which has till date not been resolved with computer simulation studies. It is, therefore, of some interest to demonstrate, in at least one situation, that Derjaguin's analysis is indeed exact in the limit of large colloid radius R.

Figure 10 draws a state in which the actual colloid particle surface is exactly one hard-sphere solvent diameter away from the planar wall (once again the boundaries represent the infinite wall–fluid repulsive potential). Rather than hard-sphere solvent, I have chosen a general fluid that, in this case, lies close to liquid–vapour

coexistence so that an annular bubble of gas has collected within the annular wedge between the colloid and the wall. The diagram is not drawn to a physical scale, since $R_c \ll R$ would be more appropriate to a Derjaguin analysis (note that R_c denotes the radius of curvature of the gas bubble, as before, not the colloid radius). The equivalent to sum rule (4) in hard-wall annular geometry [4] states that

$$\gamma = -\frac{kT}{2R}\int_R^\infty \mathrm{d}r\, r[\rho_w(r) - \rho_w(\infty)], \tag{35}$$

where the left side has been obtained from Derjaguin's large R analysis and the integral on the right side runs along the planar boundary in figure 10. In essence, Derjaguin ignores any dependence of the line tension of the annular wedge on the separation of the colloid from the wall, throughout the solvent-exclusion or depletion regime. In the special case depicted in figure 10 (i.e. drying) we can readily evaluate the right side of this expression. The left side is, in the large R limit, $\gamma_{WG} + \gamma_{LG}$, since we are close to complete drying. The insignificant wall–gas contribution is linked to the profile structure at the very centre of the annular wedge, while the majority contribution arises from the three-phase contact region where the liquid–gas interface intersects the wall (the contact angle is π but remember that we are just above saturation so that the gas-film on the planar wall is molecularly thin). Accordingly,

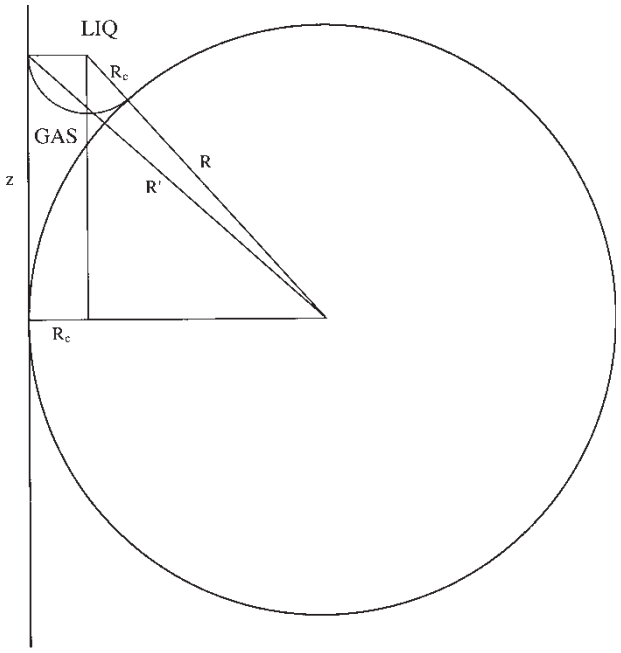

Figure 10. Geometric construction for the depletion interaction between a large spherical colloid and a planar wall. The boundary lines denote infinite wall–fluid repulsion so the diagram depicts the very beginning of the depletion regime (the colloid could move further to the left, up to one solvent diameter). By considering a hard-wall model in conjunction with a general solvent model, one can approach liquid–vapour coexistence for the solvent and thus nucleate an annular bubble of gas within the annular wedge formed by the hard walls. Note that $z^2 = (R + R_c)^2 - (R - R_c)^2 = 4RR_c$.

we can evaluate the sum rule (35) to yield the result

$$\gamma_{LG} = \frac{\Delta p}{2R}\int_R^{R'} \mathrm{d}r\, r = \frac{\Delta p(R'^2 - R^2)}{4R} = \frac{\Delta p z^2}{4R}$$
$$= \Delta p R_c. \tag{36}$$

Thus, the statistical mechanical sum rule (35), with the left side evaluated in Derjaguin's approximation, has reduced to Laplace's equation. The only physics that Derjaguin's analysis misses in the drying situation is the presence of the large radius of curvature around the annular liquid–gas surface; this is consistent with $z \gg R_c$ which is equivalent to $R \gg R_c/4$. Accordingly, there is at least one circumstance (drying of an annular wedge) where Derjaguin's analysis applies correctly to the depletion regime of colloidal science. It remains to be determined whether or not this success carries over to the case of hard sphere solvent. If so, dramatic consequences arise that cannot be described by FMDFT [4].

7. Discussion

Nanoscience is often concerned with the use of structured surfaces to manipulate small volumes of fluid (e.g. nanofluidics) or with the self-assembly of nano-particles within solution or at substrates. Such systems are becoming progressively easier to manufacture and in addition provide interesting challenges to our understanding of inhomogeneous fluids. The triangular wedge/edge model is proposed as a useful paradigm for the development of the fundamental understanding of the nano world, which can only come from incorporating statistical mechanics. There is, of course, much to be looked forwarded to with regard to the application of recent advances in non-equilibrium statistical mechanics [32]. Above, it is stressed that nanoscience already generates remarkably interesting problems for equilibrium statistical mechanics. There is a history to this work, some of which is acknowledged in Section 1, that goes back to the very beginnings of the molecular theory of capillarity [9]. Recent work has stressed the significance of the reduced dimensionality (quasi one-dimensional for a linear wedge) which implies a greater significance to fluctuation physics [8], on the negative side setting limits to the performance of nanofluidic chips, while on the positive side making it easier to devise bistable devices.

The wedge/edge sum rules and the virial equation for Young's contact angle, whose derivation was discussed in section 2, are important examples of exact results readily obtainable from statistical mechanics. The left sides of these sum rules are the thermodynamic quantities (surface tensions, interfacial torques) that experimentalists seek to measure and technologists seek to exploit. The right sides concern nothing more than the one-body structure induced on the interfacial fluid by the containing walls or colloid configurations, as is common to a wide class of virial theorems. These sum rules will thus be easy to evaluate or

to use in computer simulation experiments, or indeed in laboratory experiments capable of direct observation of the density profile structure. Density functional theory struggles with the numerical demands of complex geometry, so that exact results are important for error checking in DFT, as with simulation. Those attempting "realistic" simulations will not adopt the idealized wedge/edge models discussed here. Rather they will use coarse-grained molecular models that will inevitably generate complex non-generic geometry in the immediate vicinity of an apex. Nevertheless, the methods of generating virial theorems (section 2) apply equally to any wall–fluid model no matter how complex the geometry. Thus, for any such system one can always generate specific sum rules for the model in hand.

In Sections 3 and 4, some of the physics contained within the wedge sum rules are explored. The Derjaguin approximation proved particularly useful in understanding the physics of line tension and its angular derivative (solvation torque). A subtle issue concerning the unique definition of a line adsorption is relegated to the Appendix. Section 4 provides a sum rule analysis of classical capillarity in wedge geometry, allowing for chemically distinct walls. Due to the existence of the filling condition (figure 6), a macroscopic wedge can be filled with an arbitrary amount of liquid even though Young's contact angle at the wedge walls is non-zero. The geometric construction of figure 7 is testimony to the consistency of the wedge sum rules and the virial theorem for Young's contact angle, with each other and with Young's and Laplace's equations. Since the latter are expressions of mechanical equilibrium, figure 7 implies that the sum rules are themselves expressions of mechanical stability (typical of virial theorems and in fact inherent in the construction of figures 3 and 4—the force on the fluid due to the walls must balance the force on the walls due to the fluid).

Sections 5 and 6 illustrate some of the relevance of sum rule analyses to colloidal science. The behaviour of a solvated nano-sized colloid particle is controlled by fluid-mediated interactions arising from the structure that the colloid induces in the solvent. The solvation force on the particle is identical in form to the first wedge/edge sum rule. The moral of the "flying" wedge story is that one cannot ignore the inevitable conjunction of wedges with edges. Section 6 considers an important issue concerning annular wedge geometry, the basic geometry of colloidal physics. Very similar physics to that sketched in figure 10 applies to colloidal objects self-assembling under the influence of fluid bridges or via the standard depletion interaction.

8. Note added in proof

Equations (5) and (7) are not fully consistent because the virial process used to derive (5) has not explicitly considered the boundary condition arbitrarily far from the apex. When the thermodynamic limit is taken correctly an additional non-virial contribution to the line tension of the wedge apex is obtained. This far boundary contribution invalidates the symmetry expressed by equation (26) and ensures that the solvation torque $\partial\pi/\partial\beta$ remains non-zero at $\beta = \pi$ even for a symmetric wedge, although the correction is numerically insignificant for acute wedges and does not contribute to (27). A full derivation will be published elsewhere; J.R. Henderson. On the statistical mechanics of fluids adsorbed in chemically non-symmetric linear wedges. Preprint (2005).

Acknowledgements

It is a pleasure to thank G. Palágyi and S. Dietrich for extensive discussion concerning the physical meaning of line adsorption.

A. Appendix: Line adsorption and line tension

From the decomposition of the Grand potential defined by equation (7), we can define the line adsorption as minus the derivative w.r.t. chemical potential of the line tension; $-\partial\pi(\beta)/\partial\mu$. This obvious extension of the Gibbs adsorption equation has arisen because the wedge angle β is not dependent on the thermodynamic fields T, μ and thus one can take the derivative w.r.t. μ without affecting β. In contrast, for fluid–fluid wedges, or wall–fluid wedges, where the contact angles are functions of the bulk thermodynamic state, this relationship has to be modified [33]. Let us now calculate this derivative and thereby identify the line adsorption that is directly defined by the line tension entering into sum rule (5).

By differentiation of the Grand partition function we have

$$\frac{\partial\Omega}{\partial\mu} = -\rho V - \int \mathrm{d}\mathbf{r}[\rho(\mathbf{r}) - \rho], \tag{37}$$

where ρ denotes the bulk density arbitrarily far from the wedge walls. Using the coordinate system of figure A1 and introducing $\rho^{\pi}(z)$ to denote the planar density profile from a semi-infinite wall lying in the xy plane, we can evaluate the right side of equation (37) as

$$\begin{aligned}
\frac{\partial\Omega}{\partial\mu} &= -\rho V - 2L_y\int_0^{L_x}\mathrm{d}x\int_0^{x\tan(\beta/2)}\mathrm{d}z[\rho(x,z)-\rho] \\
&= -\rho V - 2L_y\int_0^{L_x}\mathrm{d}x\int_0^{x\tan(\beta/2)}\mathrm{d}z[\rho^{\pi}(z)-\rho] \\
&\quad - 2L_y\int_0^{L_x}\mathrm{d}x\int_0^{x\tan(\beta/2)}\mathrm{d}z[\rho(x,z)-\rho^{\pi}(z)] \\
&= -\rho V - 2L_xL_y\int_0^{\infty}\mathrm{d}z[\rho^{\pi}(z)-\rho] \\
&\quad + \frac{2L_y}{\tan(\beta/2)}\int_0^{\infty}\mathrm{d}z\,z[\rho^{\pi}(z)-\rho] \\
&\quad - 2L_y\int_0^{\infty}\mathrm{d}x\int_0^{x\tan(\beta/2)}\mathrm{d}z[\rho(x,z)-\rho^{\pi}(z)],
\end{aligned} \tag{38}$$

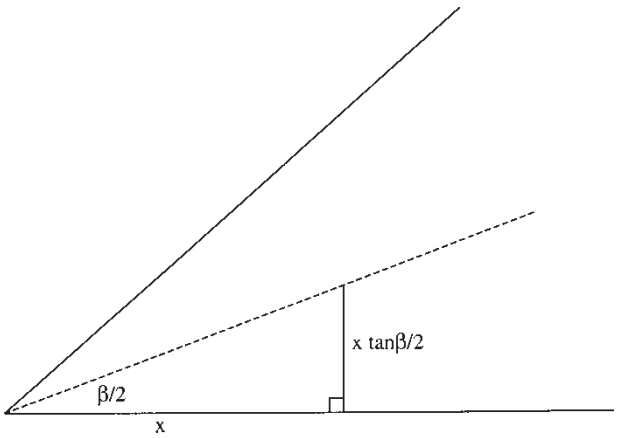

Figure A1. Coordinate system for evaluating the line adsorption of a fluid adsorbed in a linear triangular wedge.

where the thermodynamic limit $L_x \rightarrow \infty$ is taken in the upper limits of the last equality. Note that the coordinate system (figure A1) has enforced a particular choice of far boundary condition, that will continue to influence the result even when the thermodynamic limit is taken; this issue shall be looked upon, shortly. Firstly, note that direct comparison of equation (38) with equation (7) gives us the line adsorption

$$\frac{-\partial\tau(\beta)}{\partial\mu} = -\frac{2}{\tan(\beta/2)}\int_0^\infty \mathrm{d}z z[\rho^\pi(z)-\rho] + 2\int_0^\infty \mathrm{d}x \int_0^{x\tan(\beta/2)} \mathrm{d}z[\rho(x,z)-\rho^\pi(z)]. \quad (39)$$

The final term of this result arises directly from the difference between the density profile in the wedge and the density profile of a semi-infinite wall–fluid interface. The first term on the right side has arisen because in the region of the apex, a wedge-shaped portion of fluid is missing in the wedge system (figure A1). The appendix of ref. [11] explains in detail that the prefactor in front of this unexpected term is altered by different choices of far boundary condition; there is even one choice that removes it altogether. Since sum rule (5) does not suffer from an ambiguity due to the choice of far boundary condition, it follows that we must ask the question which expression for the line adsorption is associated with the sum rule; i.e. which expression belongs to the isolated wedge. Let me denote the controversial term, the first term on the right of equation (39), as the fluid–wedge term, since it is the line adsorption belonging to a wedge-shaped portion of a semi-infinite wall–fluid interface. Consider the Grand potential of a rectangular-shaped subsystem of a planar wall–fluid interface. Directly analogous to equation (7) this subsystem has a bulk $-pV$ term and a single γA interfacial contribution. However, imagine instead that, say, the right boundary of this subsystem is tilted with respect to the normal to the wall. This related subsystem now contains a wedge-shaped region of fluid, within the influence of the planar wall, which demands an additional term be included in the Grand potential of the subsystem. In fact, readers should have no difficulty confirming that this fluid–wedge contribution is precisely of the form appearing immediately on the right of equation (39). Now we can see the physical significance of the perpendicular far boundary condition assumed in figure A1; namely, if we chose any other orientation for the far boundary then, by analogy with the planar subsystem discussed above, we would have to modify equation (7) to include the fluid–wedge line tension term that would have been introduced arbitrarily far from the wedge apex.

The above argument is persuasive that equation (39) is indeed the true line adsorption of an isolated wedge. Nevertheless, it is perhaps wise to check this subtle argument by analytic evaluation in the Derjaguin approximation. For a planar pore (subscript pp) there can be no doubt that the far boundaries must be taken to lie perpendicular to the pore walls (see figure 2(b) but in the absence of two-phase coexistence within the pore), to avoid spurious fluid–wedge terms in the Grand potential

$$\Omega_{\mathrm{pp}} = -pV + (2\gamma + \Phi(h))L_xL_y. \quad (40)$$

The total adsorption in the pore follows from

$$\begin{aligned}\frac{\partial\Omega_{pp}/A}{\partial\mu} &= -\rho h - \int_0^h \mathrm{d}z[\rho(z;h)-\rho] \\ &= -\rho h - 2\int_0^{h/2} \mathrm{d}z\{[\rho^\pi(z)-\rho]+[\rho(z;h)-\rho^\pi(z)]\} \\ &= -\rho h - 2\int_0^\infty \mathrm{d}z[\rho^\pi(z)-\rho] \\ &\quad + 2\int_{h/2}^\infty \mathrm{d}z[\rho^\pi(z)-\rho] - 2\int_0^{h/2}\mathrm{d}z[\rho(z;h)-\rho^\pi(z)].\end{aligned} \quad (41)$$

Then comparison with equation (40) identifies

$$\frac{\partial\Phi(h)}{\partial\mu} = 2\int_{h/2}^\infty \mathrm{d}z[\rho^\pi(z)-\rho] - 2\int_0^{h/2}\mathrm{d}z[\rho(z;h) - \rho^\pi(z)]. \quad (42)$$

In particular, let us integrate this expression w.r.t. h, from zero to infinity, to obtain an expression for the quantity W defined in equation (18) that appears in Derjaguin analyses of the solvation of a wedge and other colloidal problems:

$$\frac{\partial W}{\partial\mu} = 4\int_0^\infty \mathrm{d}z z[\rho^\pi(z)-\rho] - 2\int_0^\infty \mathrm{d}h\int_0^{h/2}\mathrm{d}z[\rho(z;h) - \rho^\pi(z)]. \quad (43)$$

If we now translate to the Derjaguin analysis of the wedge (figure 5(a) oriented as in figure A1), then $h/2 \rightarrow x\tan(\beta/2)$ and $\rho(z;h) \rightarrow \rho(x,z)$. Accordingly, the two terms on the right of equation (43) map directly onto the line adsorption result (39), to yield (in this Derjaguin approximation)

$$\frac{\partial \tau(\beta)}{\partial \mu} \rightarrow \frac{1}{2\tan(\beta/2)} \frac{\partial W}{\partial \mu}. \qquad (44)$$

This expression is not quite the same as equation (19), instead it is the analogous result obtained in ref. [21] from the Derjaguin approximation applied directly to the Grand potential (rather than the solvation torque). This, of course, is precisely what is required to demonstrate within the Derjaguin approximation that equation (39) is the true line adsorption of a hypothetical isolated wedge. Note, for example, that the mysterious fluid–wedge term in the line adsorption appears naturally from the planar pore system, the first term on the right of equation (42), due to the excluded volume of the pore walls (when this is integrated over all values of h then one is calculating the missing adsorption in the region of a wedge apex). One might alter the prefactor of this term by changing the path integral of the Derjaguin analysis (of length h) but many such choices would be wildly unphysical and all allowable choices reduce to the same result for an acute wedge. Since the fluid–wedge term in equation (39) is a divergent function of β in this limit, it cannot be ignored.

References

[1] N.K. Adam. *The Physics and Chemistry of Surfaces*, pp. 180–181, Clarendon Press, Oxford (1930).
[2] D. Quéré. Rough ideas on wetting. *Physica A*, **313**, 32 (2002).
[3] B.V. Derjaguin. Untersuchungen über die Reibung und Adhäsion, IV. Theorie des Anhaftens kleiner Teilchen. *Kolloid-Z*, **69**, 155 (1934).
[4] J.R. Henderson. Depletion interactions in colloidal fluids: statistical mechanics of Derjaguin's analysis. *Physica A*, **313**, 321 (2002) and references therein.
[5] M. Kinoshita. Spatial distribution of a depletion potential between a big solute of arbitrary geometry and a big sphere immersed in small spheres. *J. Chem. Phys.*, **116**, 3493 (2002).
[6] R. Shuttleworth, G.L.J. Bailey. Interaction of water and porous materials. The spreading of a liquid over a rough solid. *Discuss. Farad. Soc.*, **3**, 16 (1948).
[7] A.B.D. Cassie. Contact angles. *Discuss. Faraday Soc.*, **3**, 11 (1948).
[8] A.O. Parry, A.J. Wood, C. Rascón. Wedge filling, cone filling and the strong fluctuation regime. *J. Phys.: Condens. Mat.*, **13**, 4591 (2001) and references therein.
[9] J.S. Rowlinson, B. Widom. *Molecular Theory of Capillarity*, Clarendon Press, Oxford (1982).
[10] J.R. Henderson. Statistical mechanics of fluids adsorbed in planar wedges: finite contact angle. *Phys. Rev. E*, **69**, 061613 (2004).
[11] G. Palágyi, S. Dietrich. Critical adsorption and Casimir torque in wedges and at ridges. *Phys. Rev. E.*, **70**, 046114 (2004).
[12] R.N. Wenzel. Resistance of solid surfaces to wetting by water. *Ind. Eng. Chem.*, **28**, 988 (1936).
[13] T. Young. An essay on the cohesion of fluids. *Philos. Trans. R. Soc.*, **95**, 65 (1805).
[14] A.B.D. Cassie, S. Baxter. Wettability of porous surfaces. *Trans. Farad. Soc.*, **40**, 546 (1944).
[15] C. Rascón, A.O. Parry. Surface phase diagrams for wetting on heterogeneous substrates. *J. Chem. Phys.*, **115**, 5258 (2001).
[16] R. Lipowsky. Structured surfaces and morphological wetting transitions. *Interface Sci.*, **9**, 105 (2001) and references therein.
[17] P. Concus, R. Finn. On the behavior of a capillary surface in a wedge. *Proc. Natl Acad. Sci.*, **63**, 292 (1969).
[18] Y. Pomeau. Wetting in a corner and related questions. *J. Colloid. Interf. Sci.*, **113**, 5 (1986).
[19] E.H. Hauge. Macroscopic theory of wetting in a wedge. *Phys. Rev. A*, **46**, 4994 (1992).
[20] A. Milchev, M. Muller, K. Binder, D.P. Landau. Wedge filling and interface delocalization in finite Ising lattices with antisymmetric surface fields. *Phys. Rev. E*, **68**, 031601 (2003).
[21] J.R. Henderson. Solvation of a wedge. *Physica A*, **305**, 381 (2002).
[22] J.R. Henderson. Interfacial statistical geometry: fluids adsorbed in wedges and at edges. *J. Chem. Phys.*, **120**, 1535 (2004).
[23] M.M. Bakri. The stress tensor in the surface layer of a classical fluid. *Physica*, **32**, 97 (1966).
[24] M.J.P. Nijmeijer, J.M.J. van Leeuwen. Microscopic expressions for the surface and line tension. *J. Phys. A*, **23**, 4211 (1990).
[25] P. Bryk, R. Roth, M. Schoen, S. Dietrich. Depletion potentials near geometrically structured substrates. *Europhys. Lett.*, **63**, 233 (2003).
[26] J.R. Henderson. Statistical mechanical sum rules. In *Fundamentals of Inhomogeneous Fluids*, D. Henderson (Ed.), Marcel Dekker, New York (1992), Chap. 2.
[27] J.O. Indekeu. Line tension near the wetting transition: results from an interface displacement model. *Physica A*, **183**, 439 (1992).
[28] B.V. Derjaguin, N.V. Churaev. Properties of water layers adjacent to interfaces. In *Fluid Interfacial Phenomena*, Croxton (Ed.), p. 702, Wiley, Chichester (1986), Chap.15 and references therein.
[29] P. Jakubczyk, M. Napiórkowski. Adsorption in a nonsymmetric wedge. *Phys. Rev. E*, **66**, 041107 (2002).
[30] J.N. Israelachvili. *Intermolecular and Surface Forces*, Academic, London (1992).
[31] M. Oettel. Depletion force between two large spheres suspended in a bath of small spheres: onset of the Derjaguin limit. *Phys. Rev. E*, **69**, 041404 (2004).
[32] D.M. Carberry, J.C. Reid, G.M. Wang, E.M. Sevick, D.J. Searles, D.J. Evans. Fluctuations and irreversibility: an experimental demonstration of a second-law-like theorem using a colloidal particle held in an optical trap. *Phys. Rev. Lett*, **92**, 140601 (2004) and references therein.
[33] Y. Djikaev and B. Widom. Geometric view of the thermodynamics of adsorption at a line of three-phase contact. *J. Chem. Phys.*, **121**, 15602 (2004).